Analysis of an Aircraft Crossing the Moon

Dr. G. Innes 2024-07-26

It is amazing what can be learned from the detailed analysis of a short video recording. Here, I look at the video clip where a Newark NJ amateur astronomer captured a commercial aircraft crossing the face of the Moon.

Using a variety of techniques, I determined:

1. The video was shot at about 10:05pm on 2 October 2017
2. The observer was in Newark, New Jersey, USA
3. The Moon was at 39 degrees above the horizon and at compass heading 153 degrees (SSE)
4. The aircraft was an Airbus A330-200 (VTP88 or P2F version) with Trent 700 engines
5. It was at a cruising altitude of 33,400 feet (10,200 m)
6. The ground speed was 525 mph (845 km/h) in the direction of travel
7. It was making a gentle right turn, banking at a 13.3 degree angle away from the camera
8. It was 10.0 miles (16.2 km) from the camera
9. The flight was moving through the compass heading of 32.5 degrees northeast, aiming beyond New York city airspace and soon to pass over the Atlantic Ocean en route to Europe.
10. The altitude is slightly less than 35,000 feet, suggesting it has almost finished climbing after departing from a nearby city, such as Philadelphia.

From this information, I was able to show the aircraft location and flight path on the map below. I have organized the explanation of the methods I used to do this into sections:

A) Aircraft Identification and Geometry
B) Lunar Observations
C) Basic Orientation and 3-D Trigonometry
D) Calculations

Fig. 1 Moon and Airbus A330-200 silhouette, 2017-10-02 10:05pm EDT.
(Video credit: Richard2maria, "**BUt it's not there!**", video duration 0:34
https://www.youtube.com/watch?v=2QWjMNrXjL4, posted October 3, 2017)

Fig. 2 Map of the New Jersey and New York city area showing the aircraft location and flightpath.

A) Aircraft Identification and Geometry

A detailed overlay of geometry is applied to the aircraft silhouette in Fig. A.1 below. This is extensively analyzed with the assistance of extra data and the formulas in Sections B, C and D.

- There are two manufacturers that make large twin-engine commercial aircraft with 4 fairings under each wing (known as Flap Track Fairings or Canoe Fairings).
- These are the Boeing 777 and the Airbus Industries A330 series.
- The fairings of the Boeing are not all equally spaced and there are no raised winglets at each wing tip, so an Airbus is the only candidate here.
- The possibilities are narrowed down by comparisons in Tables A.1 and A.2 below.

- The A330 series are differentiated by date of manufacture, length L_1 and engine size L_6.
- As of 2017, only A330-200 and A330-300 models had been delivered and were in service (https://www.airbus.com/en/products-services/commercial-aircraft/market/orders-and-deliveries and https://en.wikipedia.org/wiki/List_of_Airbus_A330_orders_and_deliveries).
- The 300 model has a longer fuselage and a longer nose section than the 200, which does not match the silhouette.
- The silhouette aircraft has the most compact engine size (Trent 700) available on A330 models.
- The aircraft is identified as an A330-200, which most closely matches the silhouette and which is the second most numerous Airbus A330, with more than 600 in service as of 2017.

- The 3-dimensional geometry is recovered from the silhouette with correction formulas presented in Section C.
- Tables A.1 and A.2 compare the corrected silhouette lengths with the dimensions of both the 200 and 300 models, expressed as ratios relative to the fuselage diameter L_5.
- In Fig. A.1, $L_{5\text{photo}} = 1.281$ cm and $L_{6\text{phtoto}} = 0.7185$ cm are tube diameters and need no correction.
- From the correction of Eqn [C.6] in subsection C.4 below, $L_{1\text{cor}} = 12.424$ cm, $L_{3\text{cor}} = 4.141$ cm,

L_{7cor} = 4.507 cm and L_{9cor} = 1.027 cm.

- From Eqn [C.11] in subsection C.4 below, L_{2cor} = 13.210 cm and L_{4cor} = 4.334 cm.
- The tail height L_{8cor} = 2.033 cm is derived from L_{8photo} in subsection C.6, since the tip is hidden in the silhouette (indicated by the dashed lines) and so must be reconstructed.

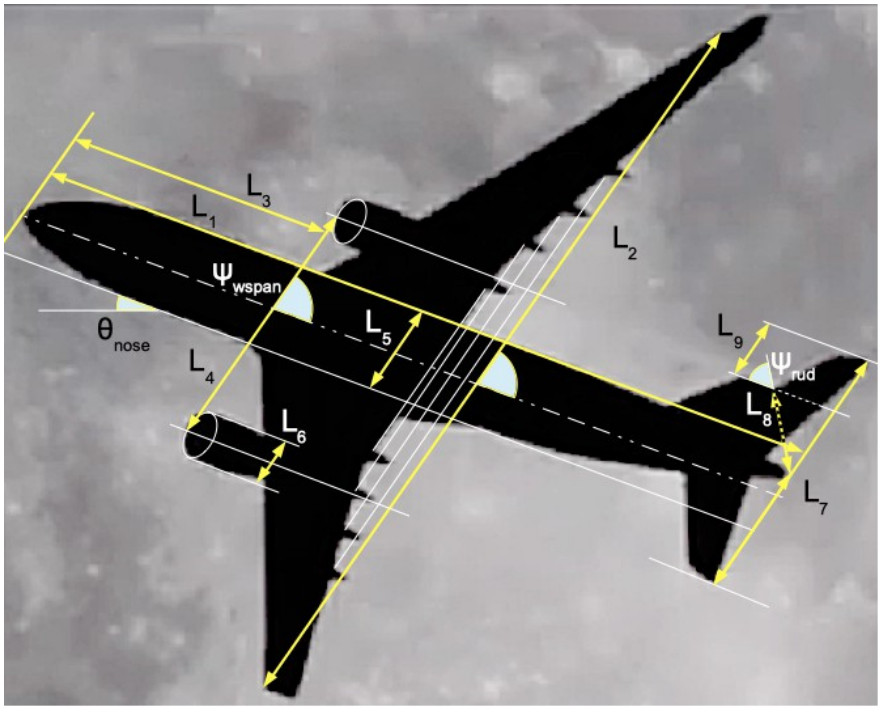

Fig. A.1 Silhouette of the aircraft against the Moon with added lines to define critical lengths. Due to the pixelated edges, the estimated error is ±0.05 cm:

L_{1photo} = 11.419 cm, aircraft overall length
L_{2photo} = 11.382 cm, wing span (less winglets)
L_{3photo} = 3.806 cm, nose-to-engine-inlet distance
L_{4photo} = 3.734 cm, engine centerline spacing
L_{5photo} = 1.281 cm, fuselage diameter
L_{6photo} = 0.7185 cm, engine diameter
L_{7photo} = 3.883 cm, tail span
L_{8photo} = 1.202 cm, tail height (reconstructed)
L_{9photo} = 0.8848 cm, tail height offset

The aircraft nose appears oriented at an angle of θ_{nose} = 20.32 degrees relative to the camera frame, the wingspan-fuselage angle appears as ψ_{wspan} = 75.37 degrees (actual is 90 degrees) and the rudder angle appears as ψ_{rud} = 58.33 degrees (actual is 90 degrees).

Aircraft	L_2/L_5	L_4/L_5	L_6/L_5	L_7/L_5
Fig. A.1 (cm, corrected)	13.210/1.281 = 10.309	4.334/1.281 = 3.382	0.7185/1.281 = 0.5607	4.507/1.281 = 3.517
A330-200 and A330-300	57.70/5.64 = 10.230 (-0.76%)	18.50/5.64 = 3.280 (-3.01%)	3.10/5.64 = 0.5496 (-1.97%)	19.40/5.64 = 3.440 (-2.20%)

Table A.1 Comparison of critical lengths (in m) for 4 common dimensions of the candidate aircraft with corrected ratios from the silhouette in Fig. A.1. The differences are expressed as percentages.

Aircraft	L_1/L_5	L_3/L_5	L_8/L_5
Fig. A.1 (cm, corrected)	12.424/1.281 = 9.696	4.141/1.281 = 3.232	2.033/1.281 = 1.586
A330-200 VTP88 L_{1+}=58.85m, L_{2+}=60.3m ε_1 = -3.01°, ε_3 = 2.65°	56.359/5.64 = 9.993 (3.06%)	18.520/5.64 = 3.284 (1.60%)	9.10/5.64 = 1.613 (1.72%)
A330-200 P2F L_{1+}=58.85m, L_{2+}=60.3m ε_1 = -3.01°, ε_3 = 2.65°	56.466/5.64 = 10.012 (3.26%)	18.520/5.64 = 3.284 (1.60%)	9.10/5.64 = 1.613 (1.72%)
A330-200 VTP93 L_{1+}=58.85m, L_{2+}=60.3m ε_1 = -3.01°, ε_3 = 2.65°	56.146/5.64 = 9.955 (2.67%)	18.881/5.64 = 3.348 (3.58%)	9.60/5.64 = 1.702 (7.31%)
A330-300 L_{1+}=63.66m, L_{2+}=60.3m ε_1 = -2.47°, ε_3 = 1.19°	61.658/5.64 = 10.932 (12.75%)	21.240/5.64 = 3.766 (16.52%)	8.60/5.64 = 1.525 (-3.87%)

Table A.2 Comparison of critical dimensions (in m) for candidate aircraft with corrected ratios from the silhouette in Fig. A.1. The differences are expressed as percentages. The best overall fit is at the top of the list, the worst is at the bottom. The total design length is L_{1+} and the full wingspan (with winglets) is L_{2+}. Parallax angles ε_1 and ε_3 are for corrections to L_1 and L_3, see subsection C.7.
(data: https://skybrary.aero/aircraft-family/a330-family, https://aircraft.airbus.com/en/customer-care/fleet-wide-care/airport-operations-and-aircraft-characteristics/autocad-3-view-aircraft-drawings, rendering: https://www.dwgsee.com/online_viewer.html)

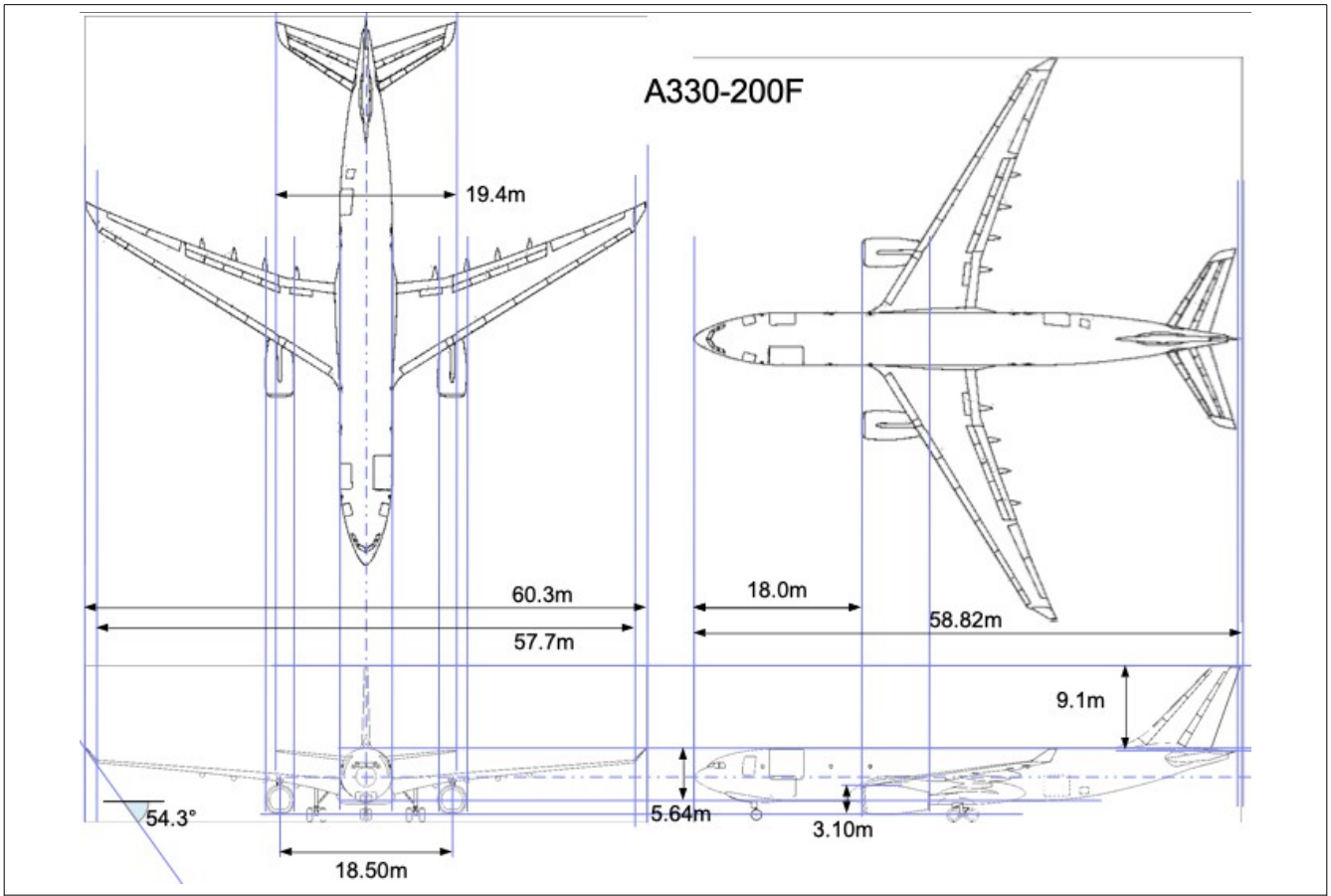

Fig. A.2 Technical drawings of the A330-200F aircraft with the smallest engine size (Trent 700).

B) Lunar Observations

- The video was posted 3 October 2017, so the observation was likely the evening of 2017-10-02.
- From other videos by the same astronomer, the location was Newark, New Jersey, USA and the telescope and camera were usually kept level with the horizon.

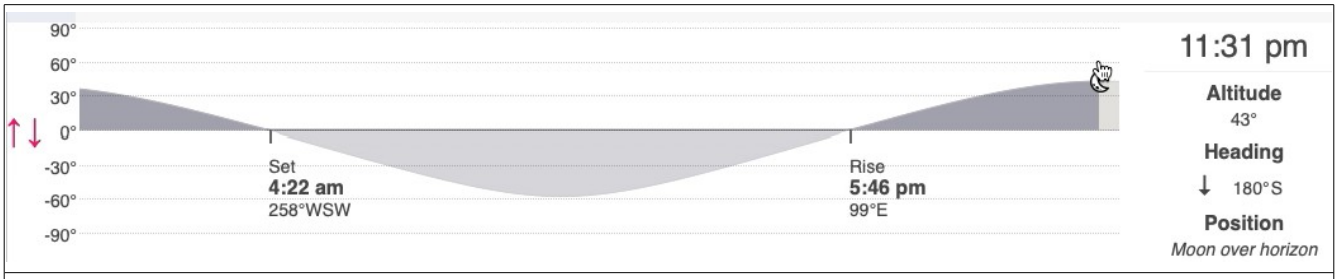

Fig. B.1 Chart of the Moon position with time for Newark, NJ, on 2 October 2017.

- From Fig. B.1, at Newark NJ on 2 October 2017, the Moon was positioned due south (180 degrees) at 11:32pm (±1 minute), with an altitude of 43±0.5 degrees above the horizon. (data: https://www.timeanddate.com/moon/).

- In Fig. B.2, the video frame of Fig. A.1 was overlaid onto a Moon reference image from Goddard Space Flight Center, which was rotated 21 degrees counter-clockwise (eastward) to be level with the horizon.
- On 2017-10-02 at 10:00pm (02:00 UT, 3 Oct 2017), the Moon appeared 0.51594 degrees in size (data: Goddard Space Flight Center, https://svs.gsfc.nasa.gov/5187).

- Due to Earth's rotation, the Moon moves westward at 4.13 minutes per degree, so the video was taken 21 x 4.13 = 87 minutes before 11:32, thus about **10:05pm** (±5 minutes, allowing ±1 degree of frame tilt).
- On 2017-10-02 at 10:05pm the Moon was **39±0.5 degrees** above the horizon at compass heading **153 degrees** SSE, seen from Newark, NJ (data: https://www.timeanddate.com/moon/).

- In Fig. B.2, using an overlay of lines to indicate the center of the Moon and critical dimensions, the angular length of the aircraft was found to be [sin(11.33°) + sin(31.05°)]/2 = 0.3561 lunar diameters.
- In Fig. B.3, from the movement between two video frames, the aircraft travelled [sin(45.48°) + sin(63.75°)]/2 = 0.8049 lunar diameters, or 2.260 times its own length, in 0.567 seconds (17 frames at 30 frames per second).
- The travel vector over 17 video frames was 17.76 degrees, indicating the nose angle of 20.32 degrees includes a “leaning back” angle of 2.56 degrees. This is a normal value for level flight.

- The aircraft was viewed from underneath at a 39 degree angle, coinciding with the Moon, potentially foreshortening the wingspan by the factor sin(39°) = 0.6293 or 62.93%
- However, the aircraft was turning right and banking at a 13.3 degree angle, changing the span foreshortening factor to sin(54.3°) or 81.21% (from analysis in Sections C and D below).

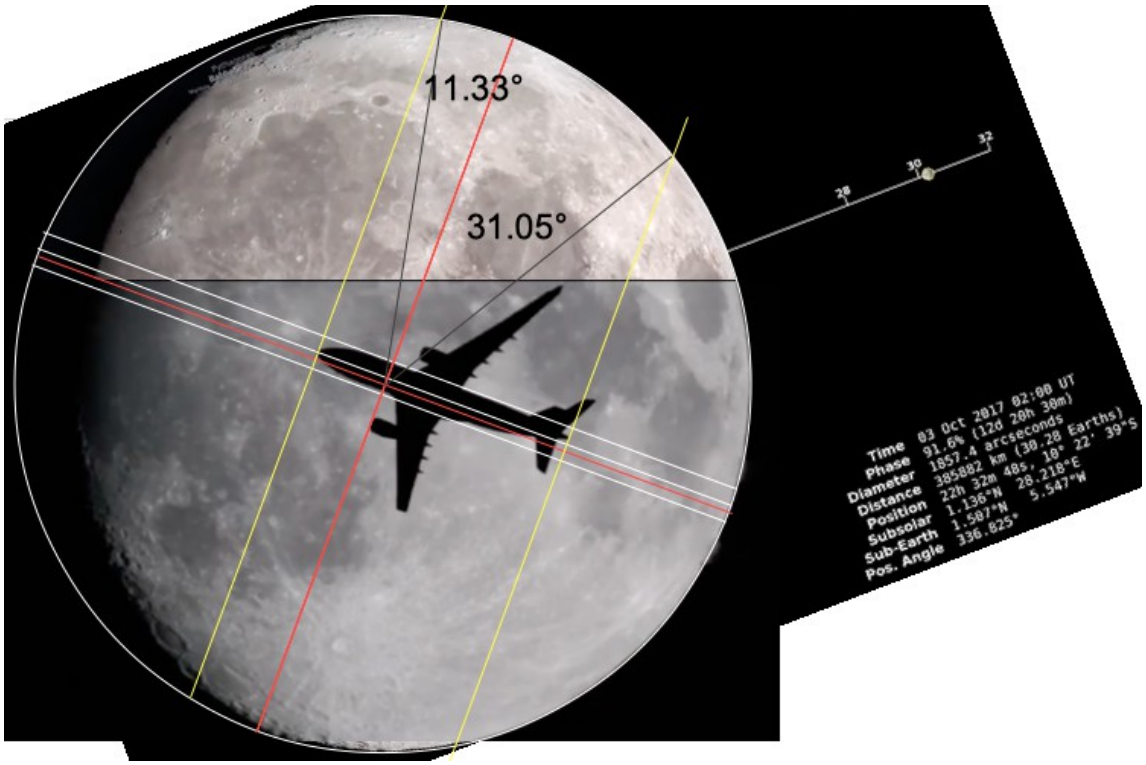

Fig. B.2 Composite image of the aircraft silhouette with the Moon reference image from Goddard Space Flight Center for 02:00 UT 3 October 2017 (10pm EDT 2 October 2017). The aircraft length is compared with the apparent size of the Moon using an overlay of geometry.

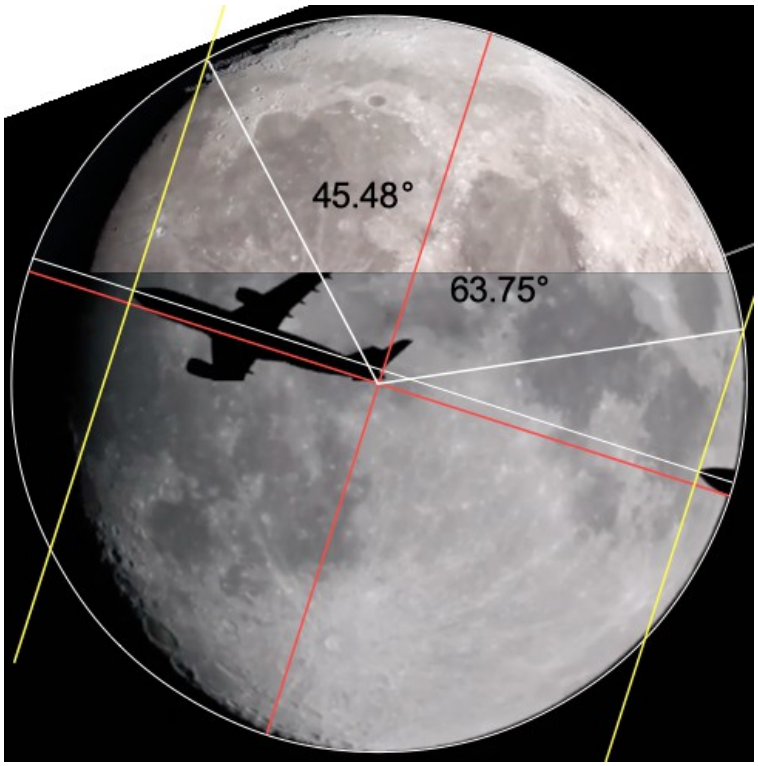

Fig. B.3 Composite image of the beginning and ending video frames of the aircraft transit of the Moon, including the reference image from Goddard Space Flight Center. The aircraft travel vector (speed and direction) is compared with the apparent size of the Moon using an overlay of geometry.

C) Basic Orientation and 3-D Trigonometry

In addition to the angle-of-view α of the objects seen through the telescope, there are 3 angles that define aircraft orientation relative to the ground-based observer. These are the azimuth angle φ, the heading angle θ and the banking angle β.

Trigonometric relationships are presented below step-by-step to allow corrected aircraft dimensions to be obtained from the photographed silhouette. It is assumed the craft is in level flight (neither climbing nor descending) and is banking in a shallow turn.

The "section view" concept from technical drawings is used here to convey the three-dimensional geometry in two-dimensional formats. The corrections to the silhouette lengths are developed one dimension at a time, leading to the final formulas.

Since the differences between aircraft models can be subtle, greater certainty of the exact model in Fig. A.1 is achieved by fine-tuning two of the aircraft dimensions. Due to the parallax effect, L_1 and L_3 are shifted slightly in Fig. A.1, since the silhouette measurement points are not strictly in-line with the fuselage centerline. Correction formulas using the parallax angles ε_1 and ε_3 are derived.

C.1 Angle-of-view α

The video was taken through a telescope with an angle-of-view α slightly wider than the full Moon. Fig. C.1 shows the aircraft half-length b and the distance from the camera L is related to the angle-of-view by the trigonometric equation:

$$L = 2b \cot(\alpha) \qquad [C.1]$$

This allows scaling of the projected (silhouetted) aircraft dimensions relative to the known size of the Moon.

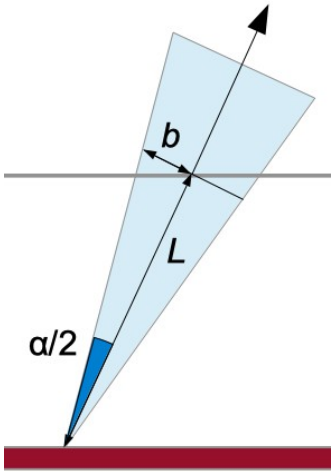

Fig. C.1 The trigonometric relationship between the telescope angle-of-view α, aircraft half-length b and distance L is $\tan(\alpha/2) = b/L$, or $L = 2b \cot(\alpha)$ if α is very small.

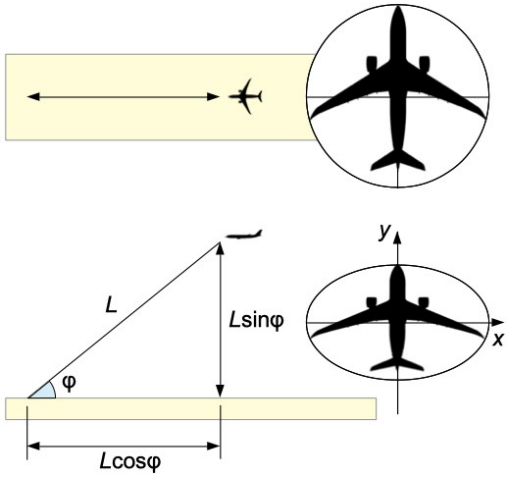

Fig. C.2 Trigonometric relationship between aircraft distance L from the observer and altitude $L\sin\varphi$. The ground (map) distance from the observer is $L\cos\varphi$. Circular inset shows aircraft silhouette from directly underneath. Elliptical inset shows observer's foreshortened view.

C.2 Azimuth Angle φ

Fig. C.2 shows the azimuth angle φ of the aircraft as seen from both the side (elevation view) and from below (plan view). The aircraft altitude is $L\sin\varphi$ and the ground (map) distance from the observer is $L\cos\varphi$, where L is the straight line distance from the camera.

Many modern aircraft have a length that is similar to the wingspan, so a single circumscribed circle will touch both the wingtips and at least one end of the fuselage. This provides a convenient reference shape for the analysis below.

From Section B, the observer was viewing the aircraft from below at an angle of φ = 39 degrees, coinciding with the azimuthal position of the Moon. The insets of Fig. C.2 indicate the ground-based observer sees the reference circle as an ellipse, foreshortening the shape of the aircraft. The definition of the ellipse is:

$$1 = X^2 + Y^2 \qquad [C.2]$$

where $X = x/a$ and $Y = y/b$ and the ellipse semi-axial lengths are a and b. If the circle has radius a, the distortion due to the angle φ means the other elliptical semi-axis b is foreshortened to $b = a\sin\varphi$.

The circle can be mapped onto the x-y coordinates of the ellipse by the equations:

$$x_{\text{ellipse}} = x_{\text{circle}} \qquad [C.3]$$
$$y_{\text{ellipse}} = y_{\text{circle}}\sin\varphi \qquad [C.4]$$

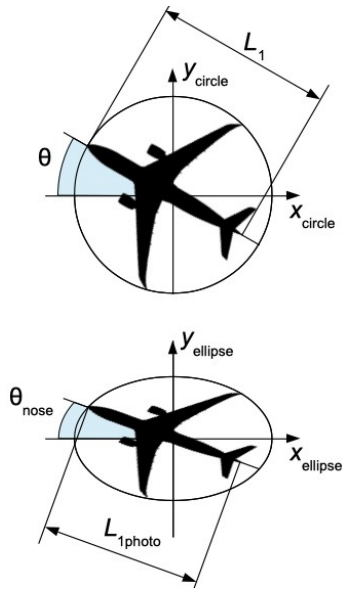

Fig. C.3 A comparison of actual heading angle θ and length L_1 (circle) with nose angle θ_{nose} and L_{1photo} (ellipse) measured in the photograph. The aircraft is shown here with no banking angle.

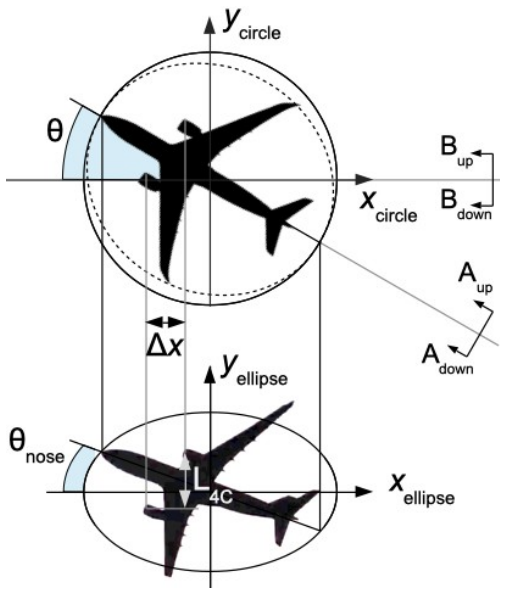

Fig. C.4 The dashed ellipse indicates the banked plane of the aircraft. The x-component of the engine spacing Δx is unchanged in the projected (lower) ellipse. Two section views A and B in Fig. C.5 provide details of the banking angle β.

C.3 Heading Angle θ

Within the circumscribed circle, the aircraft may point in any direction θ, Fig. C.3. Due to the tubular nose shape of the aircraft, the fuselage diameter appears the same regardless of the banking angle β.

Within the ellipse, the observer will see a distorted angle θ_{nose}, which is related to the actual direction θ by:

$$\theta = \text{atan}(\tan\theta_{nose}/\sin\varphi) \qquad [C.5]$$

where $\tan\theta = y_{circle}/x_{circle}$ and $\tan\theta_{nose} = y_{ellipse}/x_{ellipse} = y_{circle}\sin\varphi/x_{circle} = \tan\theta\sin\varphi$ are from Eqns [C.3] and [C.4].

From the Pythagorean theorem and Fig. C.3, the true aircraft length L_1 may be related to the length L_{1photo} measured from the photograph:

$$\begin{aligned} L_{1photo} &= [\Delta x^2 + \Delta y^2]^{1/2} \\ &= L_1 [(\cos\theta)^2 + (\sin\theta \sin\varphi)^2]^{1/2} \\ L_1/L_{1photo} &= 1/[(\cos\theta)^2 + (\sin\theta \sin\varphi)^2]^{1/2} \end{aligned} \qquad [C.6]$$

C.4 Aircraft Banking Angle β

We now consider the case where the aircraft is executing a banked turn. The banking angle β introduces a third dimension, causing changes to the projected length between the aircraft engines L_4, Figs C.4 and C.5.

The spacing between the engines is used here instead of the wingspan, since the wings do not lie in a single horizontal plane but in two planes forming a dihedral. Furthermore, the tops of the engines lie essentially in the same horizontal plane as the nose and the aircraft centerline, which simplifies the analysis.

The dashed lines indicate the plane of the aircraft at angle β to the horizontal. The horizontal and banked planes intersect along the aircraft centerline (running nose to tail).

In Fig. C.4, the change in horizontal length Δx is due to both θ and β. In the circle, the engines appear to be $L_4 \cos\beta$ apart due to foreshortening. In the ellipse, the projected distance between the engine centerlines is:

$$\Delta x = L_4 \cos\beta \sin\theta \qquad [C.7]$$

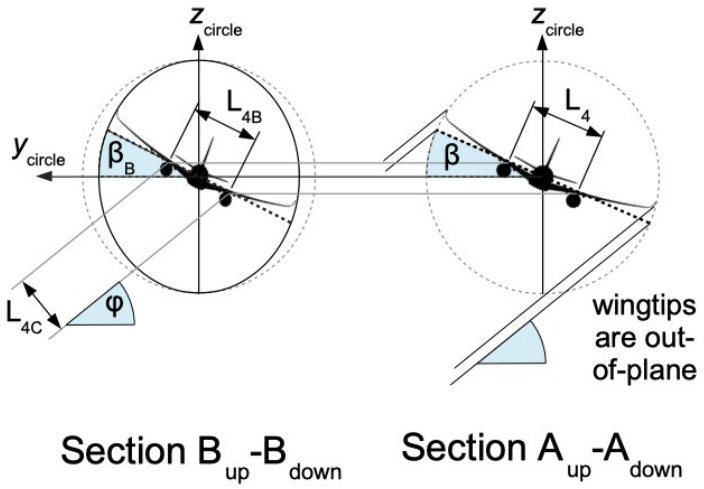

Fig. C.5 Section views A_{up}-A_{down} and B_{up}-B_{down} from Fig. C.4 show the true banking angle β and the distorted angle β_B with true length L_4 and distorted lengths L_{4B} and L_{4C}. The subscript "up" means the raised wingtip, "down" means the lowered wingtip. The aircraft is a 3-dimensional object, so the wingtips are out-of-plane here and in Fig. C.4.

The change in the vertical length component Δy is due to the 3 angles φ, θ and β. Section B_{up}-B_{down} of Fig. C.5 shows the z-component of L_4 is the same as section A_{up}-A_{down}. However, the y-component is foreshortened by the heading angle component $\cos\theta$, causing L_{4B} to be distorted. From the Pythagorean theorem:

$$\begin{aligned} L_{4B} &= [\Delta z^2 + \Delta y^2]^{1/2} \\ &= L_4 [(\sin\beta)^2 + (\cos\beta\,\cos\theta)^2]^{1/2} \end{aligned} \qquad [C.8]$$

In turn, the banking angle β is distorted by the same heading angle component. Noting that $\tan\beta = z/y$, the distorted angle becomes:

$$\begin{aligned} \tan\beta_B &= z/y\cos\theta \\ \beta_B &= \text{atan}[\ \tan\beta/\cos\theta\ ] \end{aligned} \qquad [C.9]$$

Finally, the observer sees length L_{4B} from underneath the aircraft at an angle φ. In addition to the distorted banking angle β_B, this foreshortens the y-component of the length by the combined angles, giving:

$$\begin{aligned} L_{4C} &= L_{4B} \sin(\varphi + \beta_B) \\ &= L_4[(\sin\beta)^2 + (\cos\beta\,\cos\theta)^2]^{1/2} \sin(\varphi+\beta_B) \end{aligned} \qquad [C.10]$$

Taking Δx from Eqn [C.7] and $\Delta y = L_{4C}$ from Eqn [C.10], the correction to recover the true length L_4 from that measured on the photograph L_{4photo} is based on the trigonometric relationship:

$$\begin{aligned} L_{4photo} &= [\Delta x^2 + \Delta y^2]^{1/2} \\ &= L_4 \left[(\cos\beta\sin\theta)^2 + \{[(\sin\beta)^2+(\cos\beta\cos\theta)^2]^{1/2}\sin(\varphi+\beta_B)\}^2\right]^{1/2} \\ L_4/L_{4photo} &= 1/\left[\cos^2\beta\sin^2\theta + (\sin^2\beta+\cos^2\beta\cos^2\theta)\sin^2(\varphi+\beta_B)\right]^{1/2} \end{aligned} \qquad [C.11]$$

The projected wingspan-fuselage angle ψ_{wspan} between the span of the engine intakes and the aircraft centerline is related to the 3 orientation angles by:

$$\begin{aligned} \psi_{wspan} &= \text{atan}\{\ \Delta y/\Delta x\ \} + \theta_{nose} \\ &= \text{atan}\{\ [(\sin\beta)^2+(\cos\beta\,\cos\theta)^2]^{1/2}\sin(\varphi+\beta_B)/\cos\beta\sin\theta\ \} + \theta_{nose} \end{aligned} \qquad [C.12]$$

C.5 Tail Span and Height

The tail height L_8 is obscured in the silhouette of Fig. A.1 and so must be reconstructed from the tail span L_7 and the tail offset distance L_9. The procedures are essentially the same as for subsection C.4, with the distances shown in Fig. C.6.

Section views A_{up}-A_{down} and B_{up}-B_{down} shown in Fig. C.6 indicate the same views as Fig. C.5 and so the forms of Eqns [C.8], [C.10] and [C.11] apply here to the tail span L_7:

$$\begin{aligned} L_{7B} &= [\Delta z^2 + \Delta y^2]^{1/2} \\ &= L_7 [(\sin\beta)^2 + (\cos\beta\,\cos\theta)^2]^{1/2} \end{aligned} \qquad [C.13]$$

$$\begin{aligned} L_{7C} &= L_{7B} \sin(\varphi + \beta_B) = \Delta y_{7C} \\ &= L_7[(\sin\beta)^2 + (\cos\beta\,\cos\theta)^2]^{1/2} \sin(\varphi+\beta_B) \end{aligned} \qquad [C.14]$$

$$\begin{aligned} L_{7photo} &= [\Delta x_{7C}^2 + \Delta y_{7C}^2]^{1/2} \\ &= L_7 \left[(\cos\beta\sin\theta)^2 + \{[(\sin\beta)^2+(\cos\beta\cos\theta)^2]^{1/2}\sin(\varphi+\beta_B)\}^2\right]^{1/2} \\ L_7/L_{7photo} &= 1/\left[\cos^2\beta\sin^2\theta + (\sin^2\beta+\cos^2\beta\cos^2\theta)\sin^2(\varphi+\beta_B)\right]^{1/2} \end{aligned} \qquad [C.15]$$

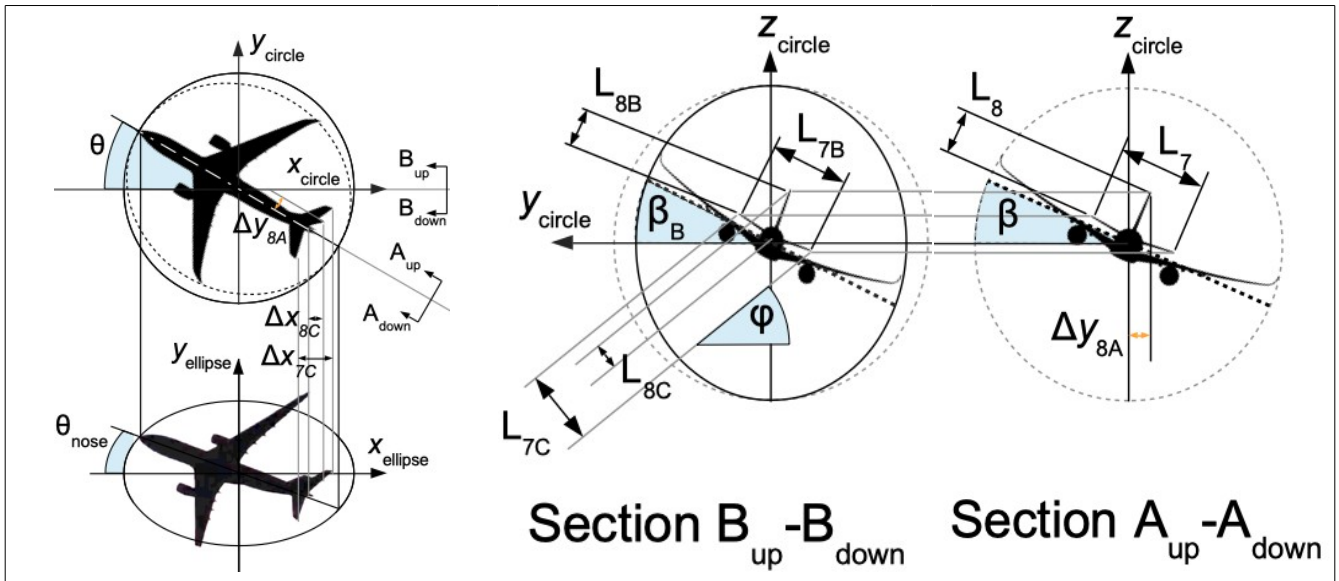

Fig. C.6 Section views A_{up}-A_{down} and B_{up}-B_{down} show the true tail lengths L_7 and L_8 and distorted lengths L_{7B}, L_{7C}, L_{8B} and L_{8C}. The x-components of L_{7photo} and L_{8photo} are Δx_{7C} and Δx_{8C}. The orange arrows show Δy_{8A} in two different views. The subscript "up" means the raised wingtip, "down" means the lowered wingtip.

Noting that the rudder is orthogonal (90°) to the tail span and that $\sin(\beta + 90°) = \cos\beta$, in section view B_{up}-B_{down} the foreshortened tail height L_{8B} is:

$$\begin{aligned} L_{8B} &= [\Delta z^2 + \Delta y^2]^{1/2} \\ &= L_8 [(\cos\beta)^2 + (\sin\beta \cos\theta)^2]^{1/2} \end{aligned} \quad [C.16]$$

From Fig. C.6, the tail height has a Δy_{8A} component (orange arrows) due to the banking angle:

$$\Delta y_{8A} = L_8 \sin\beta \quad [C.17]$$

In addition to this y-component, the tail height also has an x-component in both the circular and elliptical views of Fig. C.6. Similar to Eqn [C.7]:

$$\Delta x_{8C} = L_8 \sin\beta \sin\theta \quad [C.18]$$

Similar to Eqn [C.10] and noting that $\sin(\varphi+\beta+90°) = \cos(\varphi+\beta)$, the observed length component L_{8C} becomes:

$$\begin{aligned} L_{8C} &= L_{8B} \cos(\varphi + \beta_B) \\ &= L_8[(\cos\beta)^2 + (\sin\beta \cos\theta)^2]^{1/2} \cos(\varphi+\beta_B) \end{aligned} \quad [C.19]$$

Similar to Eqn [C.11], with Δx_{8C} from Eqn [C.18] and $\Delta y_{8C} = L_{8C}$ from Eqn [C.19], the correction to the tail height measurement from the silhouette is:

$$\begin{aligned} L_{8photo} &= [\Delta x_{8C}{}^2 + \Delta y_{8C}{}^2]^{1/2} \\ &= L_8 \left[(\sin\beta\sin\theta)^2 + \{[(\cos\beta)^2+(\sin\beta\cos\theta)^2]^{1/2}\cos(\varphi+\beta_B)\}^2\right]^{1/2} \\ L_8/L_{8photo} &= 1/\left[\sin^2\beta\sin^2\theta + (\cos^2\beta+\sin^2\beta\cos^2\theta)\cos^2(\varphi+\beta_B)\right]^{1/2} \end{aligned} \quad [C.20]$$

C.6 Rudder Angle and Reconstructed Tail Height

While Eqn [C.20] provides a correction to L_{8photo}, that length is obscured within the silhouette and so must be reconstructed using the rudder angle ψ_{rud}, shown in Figs C.7 and C.8. Similar to Eqn [C.12], ψ_{rud} is determined by:

$$\psi_{rud} = \text{atan}\{\ \Delta y_{8C}/\Delta x_{8C}\ \} - \theta_{nose}$$
$$= \text{atan}\{\ [(\cos\beta)^2+(\sin\beta\cos\theta)^2]^{1/2}\cos(\varphi+\beta_B)/\sin\beta\sin\theta\ \} - \theta_{nose} \qquad [C.21]$$

From Fig. C.8, the trigonometric relationships hold:

$$h = L_{8photo}\sin\psi_{rud} = (0.5L_{7photo} - L_{9photo})\sin\psi_{wspan}$$
thus the ratios: $$L_{8photo}/\sin\psi_{wspan} = (0.5L_{7photo} - L_{9photo})/\sin\psi_{rud} \qquad [C.22]$$

and so L_{8photo} may be reconstructed from L_{7photo}, L_{9photo}, ψ_{wspan} and ψ_{rud}:

$$L_{8photo} = (0.5L_{7photo} - L_{9photo})\sin\psi_{wspan}/\sin\psi_{rud} \qquad [C.23]$$

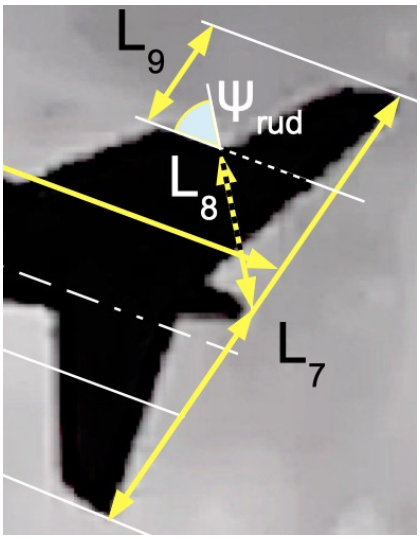

Fig. C.7 Measurements of the tail span and height.

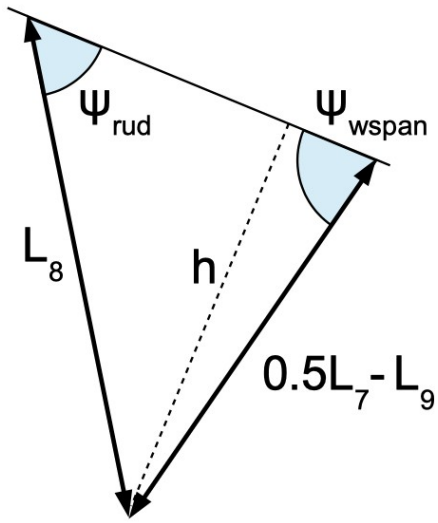

Fig. C.8 Trigonometry of the tail span and height.

C.7 Parallax Corrections

The aircraft is a 3-dimensional object, which causes parallax distortions of two lengths L_1 and L_3 seen in Fig. C.9. Their critical measurement points from the silhouette do not lie on the centerline of the fuselage, but lie at angles ε_1 and ε_3 away from the axis. The result is the appearance of parallax lengths ΔL_1 and ΔL_3.

The values of ε_1 and ε_3 depend on the model of aircraft and are listed in Table A.2 based on data from the technical drawings. The formula to calculate the parallax lengths is derived from the aligned viewing angle φ_B shown in Fig. C.9:

$$\tan\varphi_B = y/x = L\tan(\varepsilon)/\Delta L$$
$$\Delta L = L\tan(\varepsilon)/\tan\varphi_B \qquad [C.24]$$

The formulas to determine the aligned viewing angle are illustrated in Figs. C.10 and C.11 for straight-line flight (φ_A) and banked flight (φ_B), respectively:

$$\varphi_A = \text{atan}[\ \tan\varphi/\sin\theta\ ] \quad [C.25]$$
$$\varphi_B = \text{atan}[\ \tan\varphi/(\sin\theta\cos\beta)\ ] \quad [C.26]$$

Eqn [C.26] reduces to Eqn [C.25] for $\beta = 0$. Substituting into Eqn [C.24] yields:

$$\Delta L = L\tan(\varepsilon)\sin\theta\cos\beta/\tan\varphi \quad [C.27]$$

The technical dimensions for each aircraft are adjusted for comparison with the silhouette dimensions (see Fig. C.9 for illustration):

$$L \rightarrow [L + \Delta L] = L[1 + \tan(\varepsilon)\sin\theta\cos\beta/\tan\varphi] \quad [C.28]$$

Note that ε_1 is taken as a negative value, causing ΔL_1 to be negative. As a refinement, the "leaning back" flight angle ε_0 from Section B may be added to φ_B (for L_3) or subtracted (for L_1) to obtain slightly improved accuracy:

$$[L + \Delta L] = L[1 + \tan(\varepsilon)/\tan(\varphi_B \pm \varepsilon_0)] \quad [C.29]$$

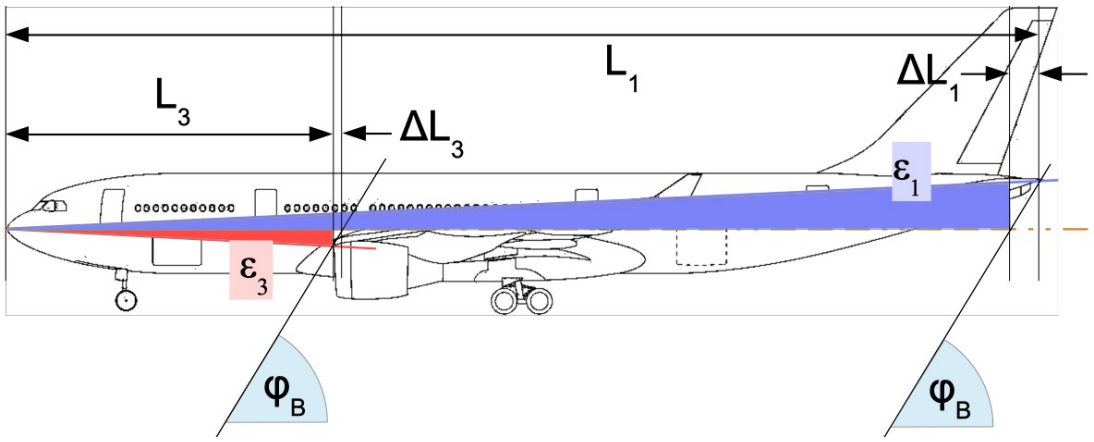

Fig. C.9 Definitions of the parallax angles ε_1 (blue) and ε_3 (red) which cause parallax lengths ΔL_1 and ΔL_3 to appear when viewed from directly below at an angle φ_B. Here, ε_1 is considered to be a negative value. Note that the definition for L_1 here and in Table A.1 is based on the photograph of Fig. A.1 and is slightly less than the total design length in the technical drawings (denoted as L_{1+}).

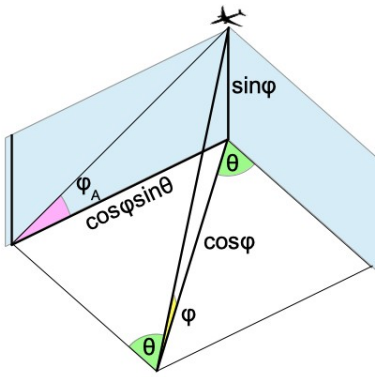

$\tan(\varphi_A) = \sin\varphi/(\cos\varphi\sin\theta)$
$= \tan\varphi/\sin\theta$

Fig. C.10 Oblique view of the aligned viewing angle φ_A along the flightpath, with aircraft in level flight. The aircraft-to-observer length is unity.

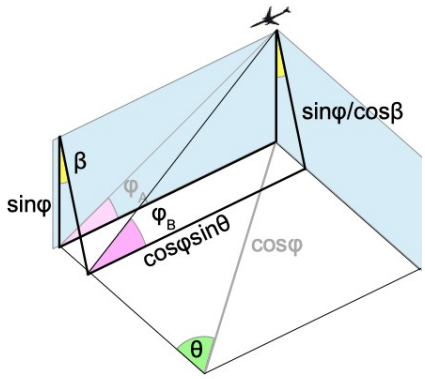

$\tan(\varphi_B) = (\sin\varphi/\cos\beta)/(\cos\varphi\sin\theta)$
$= \tan\varphi/(\sin\theta\cos\beta)$

Fig. C.11 Aligned viewing angle φ_B along the flightpath looking directly at the aircraft underside with banking angle β.

D) Calculations

The data from Sections A and B are used with the formulas and diagrams of Section C to obtain a 3-dimensional description of the aircraft in the silhouette of Fig. A.1. A spreadsheet was used to obtain the numbers below, which are rounded off. The actual errors may be several percent due to the accuracy of the available data. Numbers in **bold** typeface are directly represented in the main Section.

D.1 Orientation Angles

- From Section B, the azimuth angle **φ = 39°** is the same as the Moon at the time of observation.
- From Eqn [C.5] and the nose angle $\theta_{nose} = 20.32°$ from the silhouette of Section A, the heading angle is **θ = 30.47°**.
- From Eqns [C.9] and [C.12] and $\psi_{wspan} = 75.37°$, using an iterative process, the banking angle is **β = 13.27°**.

D.2 Length Correction Factors

- From Eqn [C.6], the correction factor $L_1/L_{1photo} = 1.0881$, affecting also L_3.
- From Eqn [C.11], the correction factor $L_4/L_{4photo} = 1.1606$, affecting also L_2, L_7, L_9.
- From Eqn [C.15], the correction factor $L_7/L_{7photo} = 1.1606$.
- From Eqn [C.20], the correction factor $L_8/L_{8photo} = 1.6913$.

D.3 Rudder Angle and Reconstructed Tail Height

- From Eqn [C.21], the rudder angle ψ_{rud} = **58.33 degrees**.
- From Eqn [C.23], the tail height L_{8photo} = **1.201 cm**

D.4 Parallax Viewing Angle

- From Eqn [C.26], the aligned viewing angle is $\varphi_B = 58.64$ degrees.
- The "leaning back" angle $\varepsilon_0 = 2.56$ degrees is used in Eqn [C.29].
- The resulting parallax corrections ΔL_1 and ΔL_3 are incorporated into the data of Table A.1.
- The A330-200 aircraft length adjusted for parallax is $L_1 + \Delta L_1 = 56.36$ m (185 ft).

D.5 Apparent Aircraft Length, Moon Comparison

- From Eqn [C.6] and subsection D.4, the foreshortened aircraft length $L_{1photo} = L_1/1.0882 = 0.919$ x 56.36m = 51.80m (170 ft).
- From Section B, the length of the aircraft appeared as 0.51594° x 0.3561 lunar diameters = 0.1837 degrees.

D.6 Camera Distance, Altitude, Ground Distance

- From subsection D.5 and Fig. C.1, cot(0.1837°) = 311.9 thus the distance from the camera was L = 311.9 x 51.80m = **16.2 km,** or **10.0 miles**.
- From Fig. C.2, the altitude was sin(39°) x 16.15 = 0.6293 x 16.15 = **10.2 km**, or **33,400 ft**.
- The ground (map) distance between camera and aircraft was cos(39°) x 16.15 = **12.6 km** (**7.80 miles**).

D.7 Aircraft Speed, Turbulent Dissipation

- From Section B, the aircraft travelled 0.8049/0.3561 = 2.260 times its length in 0.567 seconds.
- The ground speed in the travel direction was 58.82m x 2.260/0.567s = **235 m/s** (**525 mph** or **845 km/h**).
- The apparent speed across the Moon was foreshortened by the factor 91.9% (subsection D.5), so appeared to be 215 m/s (480 mph or 775 km/h).
- The turbulent twin exhaust trails vanished below detectable limits in about 5 seconds. The lingering condensate trail was too thin to block out surface details of the Moon.

D.8 Banking Radius

- While banking, the aircraft will be piloted to perform a "coordinated" or "balanced" turn. This means the centrifugal force will perfectly oppose the leaning component of gravity, so passengers will not feel the aircraft is banked.
- As a simplified formula, this means $g\sin\beta = v^2/r$, where g is mainly acceleration due to gravity (9.806 m/s^2, assuming the turn is shallow), β is the banking angle, v is the aircraft speed and r the radius of the turn about a pivot point.
- For the example here, $\beta = 13.26°$, $v = 234$ m/s and so the radius is $r = v^2/g\sin\beta$ = **24,500 m** (**15.2 miles**).

D.9 Banking Pivot Point, Travel Heading

- From the map position of the observer, the pivot point was south of New York City.
- The aircraft compass heading relative to the Moon position of 153 degrees (SSE) was 153° - 90° - 30.5° = **32.5 degrees (NE)**.
- The pivot point was 90 degrees from this compass heading, at **122.5 degrees (SE)**.
- From subsection D.8, the map distance between the aircraft and pivot point was **15.2 miles**.

D.10 True Travel Vector

- As a final detail, the aircraft actually flies in a "leaning back" configuration, which means the fuselage is at a slight angle relative to the line of flight. This provides extra lift from the body which allows the craft to operate at a higher altitude and hence fly faster in the thinner air.
- The angle of travel across the Moon as seen over 17 video frames is 17.76 degrees, 2.56 degrees different from the nose angle θ_{nose} seen in each video frame.
- If this is substituted for θ_{nose}, the calculated compass direction is reduced by 3.50 degrees (about 1% of a circle), which is within the accuracy of this study.